PROMPT NEUTRINO PRODUCTION IN A 400 GeV/c PROTON BEAM DUMP EXPERIMENT*

By T. A. Romanowski

The Ohio State University, Columbus**

(*Received June 20, 1984*)

The neutrino beam dump experiment E-613 performed at Fermilab is described and its results discussed.

PACS numbers: 14.60.Gh

1. Introduction

Direct detection of charm particles in hadronic collisions has been shown to be difficult. The charm cross section is a small fraction of the total and the lifetimes of charm particles are in the range of 10^{-12}–10^{-13} s therefore the typical distances which these particles travel before decaying are short (about 1 mm).

There are three distinctly different experimental methods which are used to detect charm particles. In the first invariant mass distributions are reconstructed from detected particles and are identified for known decays of charm particles. This method is limited by a small production charm cross section and a large number of combinatorial invariant masses which constitute backgrounds. However, in this type of experiment at CERN-ISR $D^{\pm}$ ($c\bar{d}$, $d\bar{c}$) D^0 ($c\bar{u}$, $u\bar{c}$) and Λ_c (ucd) were observed in collision at $\sqrt{s} = 62$ GeV. In the second method to observe charm bubble chambers and emulsions are used where production and decay vertices can be identified and invariant masses measured. This is an accurate method but again limited by statistics and backgrounds. A third method is to observe muons or neutrinos from the decays of charm particles produced in high energy hadronic collisions. In this so-called beam dump experiment, protons or pions are incident on a target where charm and other known types of particles are produced. Hadrons then are absorbed in the shielding around the productions target because of their long lifetimes. The lifetime difference between the particles with and without charm provides the discrimination between semileptonic decays of charm as compared to these decays of particles

* Presented at the XXIV Cracow School of Theoretical Physics, Zakopane, June 6–19, 1984.

** Address: High Energy Physics Lab., Ohio State University, 174 W 18-th Av., Columbus OH 43210, USA.

containing only u d or s quarks. The fraction of long lived particles which decay is proportional to the effective target length in which they were produced. Therefore a measurement of the number of leptons produced in targets with the same A and Z but different densities can be used to obtain the prompt leptonic component by extrapolating these measurements to the infinite target density. The prompt signal can also be obtained by subtracting from the observed lepton flux, calculated number of leptons from the decays of all known particles which are produced in the beam dump. This calculation is model dependent.

TABLE I

Summary of charm cross section results

Type	Group	$\sqrt{s}$ (GeV)	Model	$\sigma(A^{1.0})$ μb/nucleon
ν	BEBC [1]	28 pCu	$(1-x)^4$	17±4
ν	CHARM [2]	28 pCu	$(1-x)^4$	18±6
ν	CDHS [3]	28 pCu	$(1-x)^4$	14±4
μ	CCFRS [4]	26.5 pFe	indep.	22±9
hybrid B.C.	LEBC [5]	26.8 piP	$(1-x)^3$	11±5
bump hunt	LSM [6]	62 pp	flat x	1.2±0.5 mb
			$(1-x)^3$	2.4±1.0
bump hunt	CBF [7]	62 pp	flat x	1.1 mb
			$(1-x)^3$	4.2
bump hunt	ACCDHW [8]	62 pp	flat x	≈ 1 mb
bump hunt	LAS [9]	62 pp	flat x	≈ 1 mb

TABLE II

Summary of ν_e/ν_μ and $\bar{\nu}_\mu/\nu_\mu$ results

Type	Group	P_{lab} (GeV)	$\bar{\nu}_\mu/\nu_\mu$	ν_e/ν_μ
1977				
ν	BEBC [1]	400 pCu		
ν	CDHS [3]	400 pCu	existence of prompt flux	
ν	Gargemelle [10]	400 pCu		
1979				
ν	BEBC [1]	400 pCu	0.79±0.62	0.59±0.53
ν	CHARM [2]	400 pCu	1.3 ±0.6	0.48±0.16
ν	CDHS [3]	400 pCu	0.46±0.21	0.64±0.22
μ	CCFRS [4]	350 pFe	1.3 ±0.3	—
1982				
ν	BEBC	400 pCu	1.22±0.73	1.35±0.69
ν	CHARM	400 pCu	0.84±0.18	0.57±0.11±0.07
ν	CDHS	400 pCu	0.80±0.20	0.83±0.13±0.12
μ	CCFRS	350 pFe	1.1 ±0.2	—

Beam dump experiments were pursued at CERN and Fermilab. At CERN the neutrino beam dump experiment was performed in three different detectors. Two of these were electronic detectors and the third one was a bubble chamber. The detectors were located 800–900 m away from the beam dump and detected neutrinos were in a small solid angle. The results from these detectors are summarized in Tables I and II. The ratios of observed neutrino fluxes $\bar{\nu}_\mu/\nu_\mu$ and ν_e/ν_μ were different from unity in some of the detectors (see Table II) which in the case of $\bar{\nu}_\mu/\nu_\mu$ may imply a significant contribution from decays of Λ_c and D's but the ratio of ν_e/ν_μ different from unity would point to the violation of μ-e universality or would require a large production of F particles.

Model dependent calculations of the observed charm production have not shown uniform agreement with the data over the observed energy range [11–23].

The somewhat surprising results from CERN experiments motivated neutrino beam dump experiment E-613 at Fermilab which was performed in the M-2 beam line in the meson area (Fig. 1). In this experiment we have measured the prompt production of ν_μ, $\bar{\nu}_\mu$ and the ν_e, $\bar{\nu}_e$ neutrinos in tungsten, copper and beryllium targets. We determined from these data the total and differential production cross sections for $D\bar{D}$ production and its A dependence. We also verified the μ-e universality in charm decays and finally set some limits on the mass and decays of supersymmetric particles.

The detector in this experiment subtended a large solid angle from 0–37 mr which allowed for simultaneous detection of neutrinos in this angular region. A particular care was taken to monitor the incident proton beam and prevent it from scraping i.e. creating prompt neutrino sources outside of the beam dump. A short distance of 56 m between the beam dump target and the neutrino detector and the use of active and passive shielding around the dump maximized the prompt neutrino flux relative to the non prompt one.

E613 COLLABORATION

University of Michigan —

R. C. Ball, C. T. Coffin, H. R. Gustafson, L. W. Jones, M. J. Longo, T. J. Roberts, B. P. Roe, E. Wang

Istituto Nazionale di Fisica Nucleare —

C. Castoldi, G. Conforto

Ohio State University —

M. B. Crisler, J. S. Hoftun, T. Y. Ling, T. A. Romanowski, J. T. Volk

University of Washington —

S. Childress

University of Wisconsin —

M. E. Duffy, G. K. Fanourakis, R. J. Loveless, D. D. Reeder, D. L. Schumann, E. S. Smith

Fig. 1

The sketch of the experimental set-up is shown in Fig. 2. A 400 GeV/c proton beam was transported to a target holder capable of placing targets in the beam made of different density tungsten, copper and beryllium. Target station was followed by a charged particle shield consisting of 20 Tesla-meters of magnetized and 11 meters of passive iron (Fig. 3). Strongly interacting particles were absorbed and a large fraction of muons originating from the semileptonic decays were ranged out or swept away from the neutrino detector located 56 meters downstream. The magnetized iron shield was a unique feature in this experiment which allowed for a relatively short distance between the beam dump target and the detector and hence substantially increased the solid angle for neutrino detection as compared to previous experiments of this kind [1–4].

The detector consisted of a 150 metric ton calorimeter with a fiducial volume of 65 tons made up of 30 modules followed by a muon spectrometer (Fig. 4). The calorimeter modules were active targets for neutrino interactions. Each module contained 12 teflon-coated lead plates immersed in NE235 liquid scintillator. The lead plates were 6.3 mm thick to give a total of 14.4 radiation lengths, 0.5 hadron absorption length, and 105 gm/cm^2 of material per module. Vertically, the modules were separated by septa into five horizontal cells. Light from the liquid scintillator was detected by photomultiplier tubes at each end of a cell. Pairs of horizontal and vertical PWC planes were interspaced throughout the calorimeter modules to track particles in the calorimeter, sample hadronic or electromagnetic shower profiles from neutrino interactions and to aid the vertex determination for the events. The transverse dimensions of the vertex fiducial volume 2.6 × 1 m^2 and only neutrino interactions in modules 3 through 24 were used. The muon spectrometer consisted of five XYU drift chamber planes inserted between three iron toroidal magnets. The neutrino beam was centered vertically but offset 0.75 m to the left of center, which allowed the calorimeter to accept neutrinos to production angles of 37 mrad.

Upstream of the calorimeter was a triple wall of counters used to prevent triggering by incident charged particles. The apparatus was triggered when sufficient energy was deposited by neutrino events within any of 24 overlapping groups of 16 contiguous calorimeter cells. The trigger threshold and efficiency were calibrated using the electromagnetic interactions of muons. In the 1981 run the trigger efficiency was greater than 95% at 10 GeV

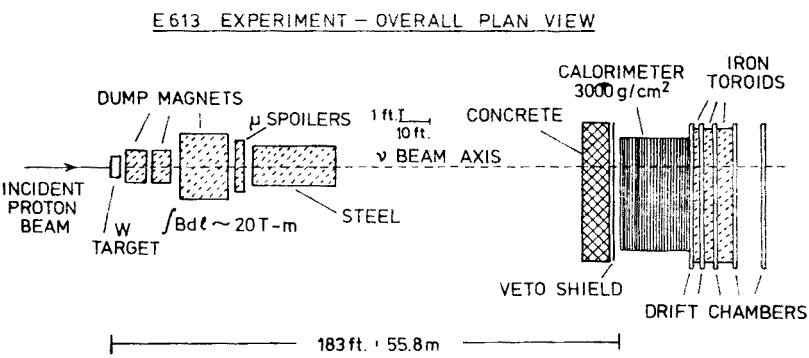

Fig. 2. E613 overall plan view

and, averaged over the fiducial volume, exceeded 50% for hadron energies greater than 6.5 GeV. In the 1982 run the definition of the energy threshold was greatly improved and a new trigger was added which only required a muon penetrating through all of the three toroids.

In order to minimize background events produced by beam scraping upstream of the target, halo monitors were placed along the beam and were calibrated by introducing foils

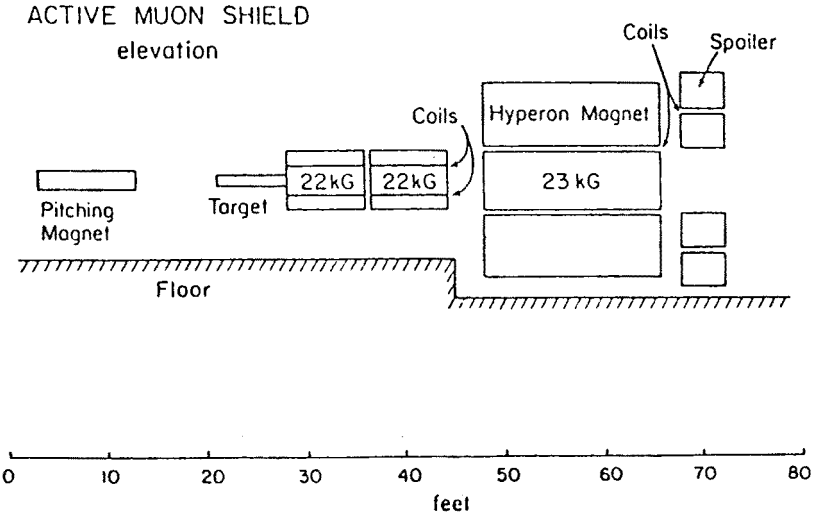

Fig. 3. The active muon shield

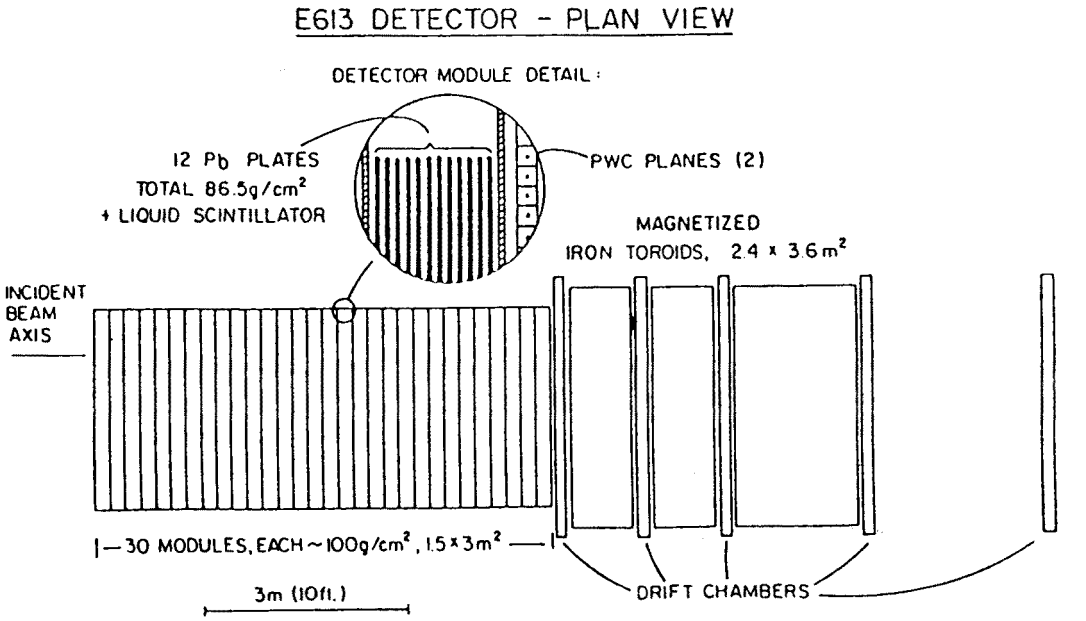

Fig. 4. E613 detector plan view

of known thickness into the beam and by varying the beam line vacuum. Spills were eliminated in which more than two halo monitors indicated twice the nominal background or target monitors indicated that the beam was not centered on the target. For the remaining spills, the background due to sources upstream of the beam intensity monitors was determined to be less than 2.0% (1% in 1982) of the prompt neutrino flux. The beam intensity devices (SWIC, SEM, etc.), vacuum windows, and air just upstream of the target introduced a larger but calculable background (5% for full and 3% for partial density tungsten in 1981 run, and about 3% and 2% in 1982 run).

The physics results obtained in this experiment will be described below.

2. *Prompt ν_μ and $\bar{\nu}_\mu$ production in Tungsten and Beryllium, and a dependence of the cross section*

Data were accumulated in two runs, one in the Spring of '81 and the other in the Spring of '82. The raw data sample taken in '82 run is shown in Table III. The partial result is based on the '81 data on the energy distribution of prompt ν_μ and $\bar{\nu}_\mu$ charged-current events,

TABLE III

Data accumulated Spring '81 and Spring '82

Target	Protons on target ($\times 10^{17}$)	Raw events		
		ν_μ	$\bar{\nu}_\mu$	0_μ
Full density W	1.37	776	276	1068
Segmented partial W	0.39	404	121	386
Be	0.77	562	133	993

the ratio of prompt $\bar{\nu}_\mu/\nu_\mu$ and the $D\bar{D}$ produced cross section was published [23] and results from the '82 data run will be presented here.

These results are based on the data collected from a full density tungsten ("hevimet") target (4.4 absorption lengths), a segmented tungsten target (3.4 absorption lengths) whose average density was one-third normal and full density beryllium target (2.6 absorption lengths). The total exposure after correcting for live time ($\sim$ 70%) and eliminating bad beam spills was 13.5×10^{16} protons on the full density W target, 3.9×10^{16} on the partial density W target and 7.7×10^{16} on the Be target.

Charged current ν_μ and $\bar{\nu}_\mu$ interactions have an outgoing μ which provides an unambiguous signal in the detector. We required that the muon pass through at least four drift chamber superplanes and that the event have a total energy greater than 20 GeV. The estimated overall efficiency (scan and muon reconstruction) for finding muon charged current events was 96%. The average acceptance of the detector for neutrino interactions with $E_\nu > 20$ GeV within the fiducial volume was calculated by several methods to be 0.6 using the measured neutrino structure functions [24, 25].

The target densities corrected for finite target length are 0.93 ϱ_W and 0.38 ϱ_W for the full and partial densities, respectively. The prompt muon neutrino spectrum was determined by a bin-by-bin extrapolation and also by a constrained fit which fixed the non-prompt $\bar{\nu}/\nu$ flux ratio, $R = 0.17$, and the shape of the non-prompt energy spectra, which were calculated from the measured π, K, Λ and Σ spectra in different targets [26, 27]. The expected distributions in scaling variables x and y, after including the distortions due to acceptance, are in good agreement with the data. The energy distribution of muon neutrinos as a function of energy and $P_\perp$ are shown in Fig. 5 and Fig. 6. From the charged current

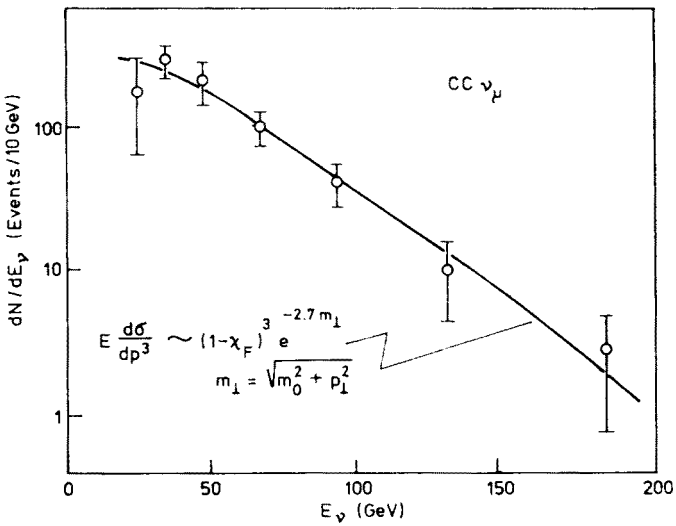

Fig. 5. Charged current muon events vs E_ν

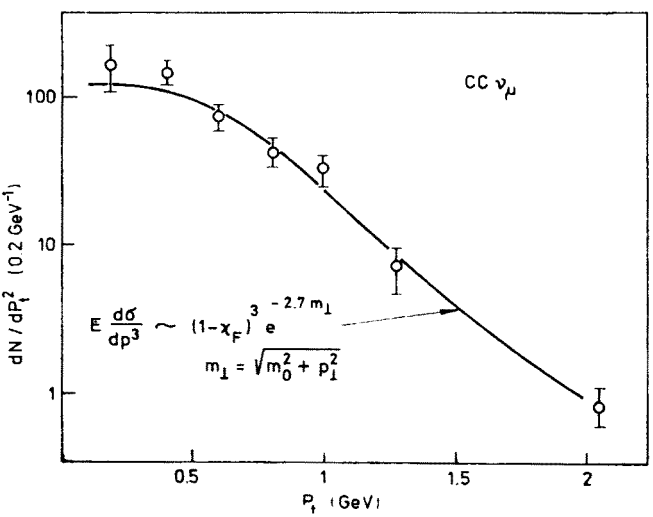

Fig. 6. Charged current muon events vs P_t

muon data an invariant $D\bar{D}$ cross section can be obtained using the accepted parametrization:

$$\frac{d^3\sigma}{dp^3} \propto (1-x)^n \exp(-am_\perp),$$

where x is the absolute value of the Feynman x and $m_\perp = (p_\perp^2 + m_0^2)^{1/2}$. The best fit to the single component ($D\bar{D}$) in that parametrization $n = 3.0$ $a = 2.7$ group

$$\sigma(D\bar{D}) = 101 \pm 14 \text{ μb/nucleon for } A^{2/3} \text{ dependence}$$
$$\text{and } \sigma(D\bar{D}) = 18 \pm 2.5 \text{ μb/nucleon for } A^1 \text{ dependence.}$$

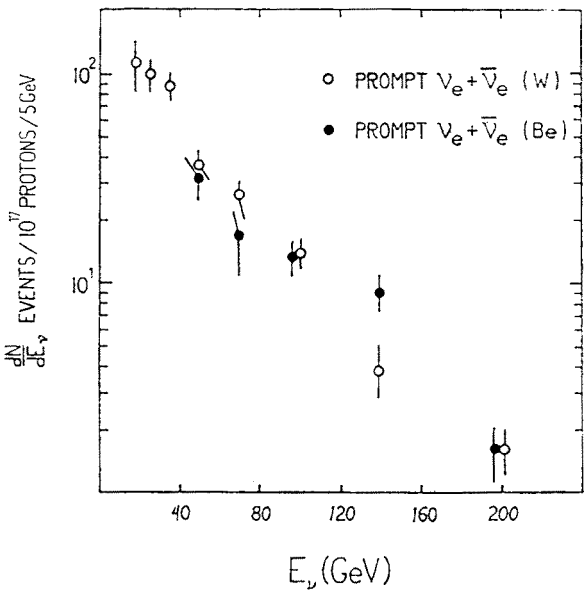

Fig. 7. Prompt ν_e energy distributions for tungsten and beryllium targets

The two components fit for production of $\Lambda_c^+\bar{D}$ with $n = 1$ and $D\bar{D}$ with $n = 3.6$ and $A^{2/3}$ yields $\sigma(D\bar{D}) = 120 \pm 52$ μb/nucleon and $\sigma(\Lambda_c^+\bar{D}) = 26 \pm 77$ μb/nucleon. Limits on the product of the F production cross section and the branching ratio of F into two body $B_2(F \to \mu\nu)$ relative to the product of the D production cross section and the branching ratio $B_3(D \to xe\nu)$ is 0.03 with 90% confidence limit. The ratio of prompt $\bar{\nu}_\mu/\nu_\mu = 1.12 \pm 0.24 \pm 0.17$. The prompt ν_e energy distribution in tungsten and beryllium are shown in Fig. 7. Assuming that the charm cross section is of the form

$$\sigma_{\text{charm}} = \sigma_c A^\zeta$$

and taking the total absorptive cross section of protons on nuclei to be

$$\sigma_T = \sigma_0 A^\alpha,$$

where $\sigma_0 = 38.6 \pm 1.50$ mb and $\alpha = 0.72 \pm 0.01$

$$\zeta = \alpha + \frac{\ln (R_1/R_2)}{\ln (A_1/A_2)},$$

where R_1 and R_2 are the prompt event rate per proton on a target with atomic number A_1 and A_2 for R_2. Taking now the events with $E_\nu = 740$ Gev $\zeta = 0.73 \pm 0.05$. In hadron production of strange particles α coefficient is a function of x. The variation of ζ as a function of energy is shown in Fig. 8. The data are consistent with constant ζ.

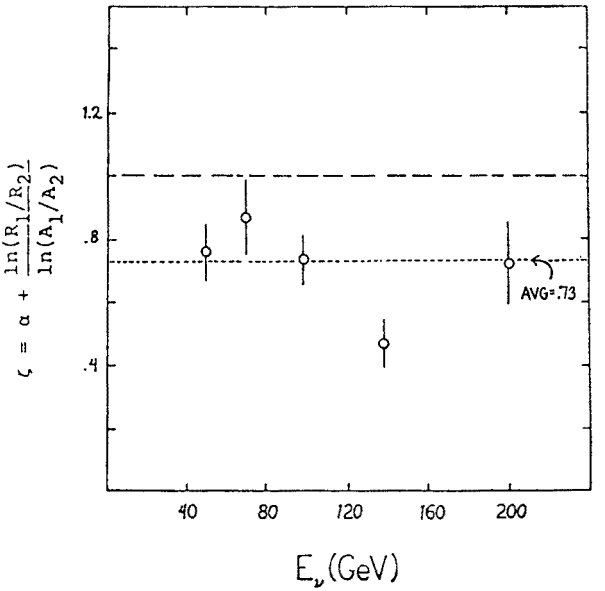

Fig. 8. *A*-dependence determination as a function of energy

3. Verification of muon-electron universality in charm decay

The selection efficiency for muonless events was determined by processing a sample of simulated NC events. This sample was created from the μ_ν CC events by removing the muon information from the raw data. These events were then randomly interleaved in the data with a frequency comparable to that of true ν events. The computer selection program retained $88 \pm 2\%$ of these events with visible energy >20 GeV. The rejected events were unbiased in visible energy and vertex position. The efficiency for retaining these simulated NC events in the scan was $95 \pm 5\%$.

The ν_e CC rate is determined from the muonless events by two independent methods: 1) subtraction of known backgrounds; and 2) use of the difference in energy deposition in the calorimeter between ν_e CC events and background NC and ν_μ events.

In the first method (see Table IV) the ν_μ NC and the ν_μ CC rates for which the muon escapes the calorimeter and does not strike the spectrometer are subtracted (geometric

TABLE IV

Compilation of results obtained in the analysis of the muonless events. Rates as a function of energy are in units of events per GeV per 10^{17} protons on target. Integral rates are in units of events per 10^{17} protons on target. Unless otherwise indicated these results are obtained with the full density tungsten target

E_ν (GeV)	Muonless rate	Background rates		ν_e rate	ν_e CC rate	ν_e CC (y_s fit)	ν_e CC prompt	ν_μ CC prompt	Asymmetry subtraction
		ν_μ CC	ν_μ NC						
20–30	26.9±1.6	6.9±0.7	5.3±0.3	14.7±1.8	11.8±1.4	11.6±2.5	10.6±1.4	9.7±3.9	0.04±0.20
30–40	20.2±1.4	3.9±0.3	3.3±0.2	13.1±1.4	11.4±1.2	8.9±2.3	10.7±1.2	9.1±2.4	0.08±0.14
40–60	10.4±0.7	2.1±0.1	1.7±0.1	6.5±0.7	5.7±0.6	5.7±1.0	5.3±0.6	7.2±1.4	−0.15±0.12
60–80	5.6±0.5	0.8±0.1	0.7±0.1	4.0±0.5	3.6±0.5	3.7±0.8	3.5±0.5	3.0±1.0	0.07±0.17
80–120	2.8±0.3	0.33±0.03	0.29±0.03	2.2±0.3	2.0±0.2	1.8±0.4	2.0±0.2	2.5±0.5	−0.14±0.12
120–160	0.71±0.13	0.08±0.02	0.07±0.01	0.56±0.13	0.53±0.13	—	0.52±0.13	0.65±0.24	−0.11±0.23
160–200	0.33±0.09	0.02±0.01	0.02±0.01	0.29±0.09	0.28±0.09	—	0.28±0.1	0.30±0.13	−0.03±0.28
>20	949±30	184±8	151±5	614±31	531±27	506±69	499±28	530±61	−0.03±0.07
>20[a]	1288±67	328±16	267±11	693±70	606±68	438±93	526±70		−0.01±0.09

[a] Partial density tungsten target.

acceptance $\sim 85\%$). These rates are determined from the measured ν_μ CC rates using the inelastic structure functions [24] and detector acceptance. Although the ratio of NC to CC interactions [29] (ν and $\bar{\nu}$ combined) in lead is 0.32, the observed ratio of detected events is 0.16 because of the restriction that $E_{\rm vis} > 20$ GeV. No distinction between prompt and non-prompt ν_μ events is necessary at this point. Only ν_e-induced events remain after the ν_μ events are removed.

The number of ν_e CC events is then determined assuming that the NC/CC ratio and the structure functions are the same as those for ν_μ [30]. Finally, the nonprompt ν_e CC events, which come from K decay, are removed ($\sim 5\%$ correction). These are obtained from direct calculation and by an independent calculation using the measured and normalized non-prompt ν_μ CC energy distribution incorporating both the differences in the decay distributions (3-body vs. 2-body) and the branching ratios [30]. The prompt ν_e CC rate in the detector is 499 ± 28 events per 10^{17} protons on target for $E_\nu > 20$ GeV. The analysis of the data obtained with the partial density target yields a corroborative result 526 ± 70 events per 10^{17} protons, albeit with a smaller signal to background ratio. The combined ν_e rate is 503 ± 26 events per 10^{17} protons.

The second method of determining the number of prompt ν_e CC events uses the characteristics of the interaction in the calorimeter. The difference between the longitudinal distribution of energy deposition of electrons and hadrons is accentuated by the use of lead in the calorimeter. A module represents 14.4 radiation lengths but only 0.5 pion absorption length, so that $> 95\%$ of an electron shower is contained within one module whereas for a typical hadronic shower the comparable length is about six modules. The observed module energies are first adjusted by interpolation of the shower curve so that the module energies are representative of an event occurring at the beginning of a module. The prompt electromagnetic energy is them almost completely contained in the first module. The procedure we use to identify ν_e CC events is to estimate the hadronic energy (including π^0) deposited in the first module using the observed energy in the subsequent modules. A ν_e CC event would usually have an observed energy in excess of this estimate, while a NC event would have an energy deposition in the first module comparable to the estimate.

The measured energy calibration of the calorimeter for electrons was $E_e^* = N(\text{nep})/5.56$, where $N(\text{nep})$ is the observed pulse area in units of the response to equivalent minimum ionizing particles. Correspondingly, the energy calibration for hadrons was $E_h = N(\text{nep})/4.40$. For ν_e CC events which contain both an electron and hadronic component the visible energy depends upon the relative contribution of each. This difference is incorporated in the estimate of the energy by defining y_s:

$$y_s = \frac{E_{\rm had}}{E_\nu} \simeq \frac{aE_{-1}}{E_{\rm tot}},$$

where E_{-1} is the observed energy calculated using the hadronic calibration and excluding the first adjusted module and where $E_{\rm tot}$ is the total energy in all modules [31]. Using data obtained with the calorimeter in a pion test beam we determined that $a \sim 2$, independent of hadronic energy. For NC events y_s should be $\simeq 1$ with a variance characteristic of the fluctuations due to the production of neutral pions in the primary interaction. For a purely

electromagnetic shower $y_s \simeq 0$ with a smaller variance. Then the neutrino energy is expressed as

$$E_\nu(y_s) = \frac{E_{\text{tot}}(\text{nep})}{5.56(1-y_s)+4.4y_s}.$$

This calculation of the neutrino energy is used throughout the analysis. The y_s distribution for hadronic background is that observed for the hadron showers of the weighted ν_μ CC events. The distribution of y_s for the $\nu_e(\bar{\nu}_e)$ events is obtained from the response of the calorimeter to an electron beam combined with the energy depositions of the weighted hadronic showers at the ν_μ CC events. The structure functions and the ratio of $\bar{\nu}_e/\nu_e$ are assumed to be the same as for ν_μ events. The y_s distribution for the full density tungsten data is shown in Fig. 9 together with the combined fit to the ν_e CC distribution and the background hadron distribution. The fitted fraction of ν_e CC events is $(53\pm7)\%$ which yields a prompt ν_e CC rate of 474 ± 69 events per 10^{17} protons, $E_\nu > 20$ GeV in good agreement with the value obtained using the subtraction method (Table IV).

The rate of prompt ν_μ CC with the same selection criteria is 530 ± 61 events per 10^{17} for $E_\nu > 20$ GeV (Table IV) [31]. We compare the two results by calculating the asymmetry $A = (\nu_e-\nu_\mu)/(\nu_e+\nu_\mu)$ of the prompt CC rates. The result is $-0.027\pm0.064\pm0.04$ for $E_\nu > 20$ GeV. The ratio of the prompt ν_e CC flux to the prompt ν_μ CC flux is $0.95\pm0.12\pm0.8$. The latter error is the systematic error due predominantly to uncertainties in the ν_μ acceptance correction. The dependence of the asymmetry on the energy and transverse momentum of the prompt neutrinos is shown in Fig. 10. The result is in agreement with muon-electron universality.

The y_s analysis can be used to search for ν_e-induced NC and/or other sources of NC-like events. If the normalization of the ν_μ background is fixed to the value expected from the

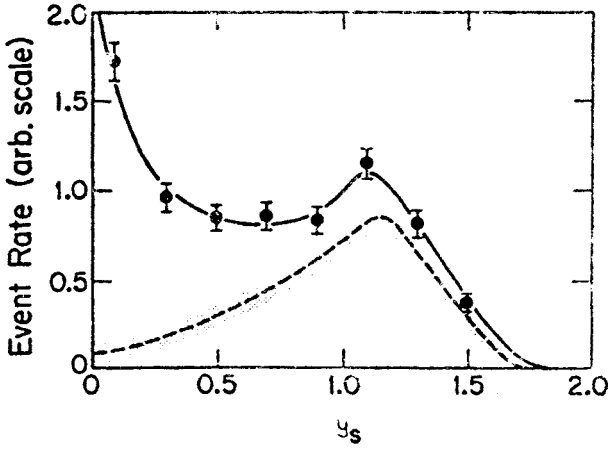

Fig. 9. The y_s distribution for the data obtained using the full density tungsten target. The solid curve is the sum of the ν_e CC distribution and the hadronic background distribution as determined in a fit to the fraction of ν_e CC present. The dashed curve is the distribution for hadron showers in ν_μ CC events normalized according to the fit

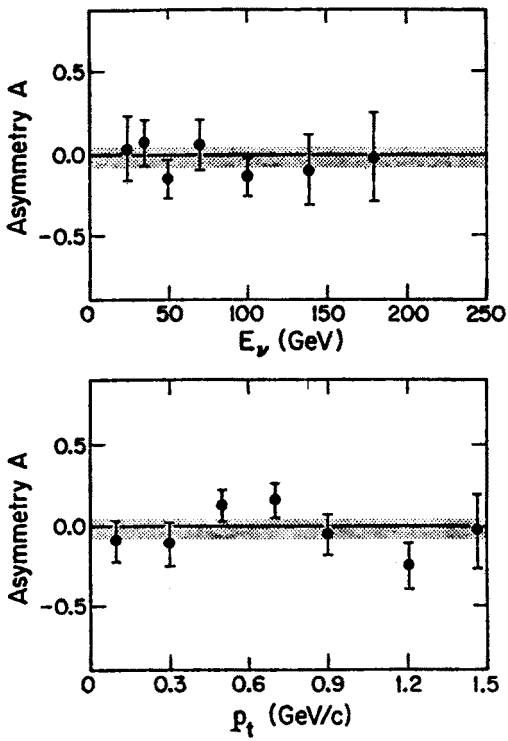

Fig. 10. The dependence of the asymmetry A on the energy and transverse momentum of the prompt neutrinos

ν_μ CC events and the y_s distribution refitted to the sum of the ν_e CC and NC distributions, it is found that the CN/CC ratio for ν_e is 0.23 ± 0.18 compared with the value 0.16 observed in ν_μ interactions. There is no significant difference which can be ascribed to a source other than the expected ν_e-induced neutral current interaction.

In summary, we find no evidence for a difference between the prompt ν_e flux and the prompt ν_μ flux observed in a beam dump experiment. We find a NC signal consistent with the universality of the neutral current interaction of ν_e and ν_μ and with the absence of other sources of prompt neutrinos.

4. Supersymmetry mass and lifetime limits from a proton beam dump experiment

The observed muonless events have been analyzed to set limits on the mass and lifetime of supersymmetric particles. For energies greater than 20 GeV the absence of an anomalous signal results in the limits: (1) assuming $\tilde{g} \to \tilde{\gamma} q\bar{q}$ dominates and the photinos are long lived ($\sigma \sim A^{0.72}$), at the 90% confidence level we find $m_{\tilde{g}} > 4.1$ GeV if $m_\phi = m_Z/2$ and $m_{\tilde{g}} > 3.1$ GeV if $m_\phi = m_Z$; (2) assuming $\tilde{g} \to g\tilde{G}$ dominates, where $\tilde{G}$ is a goldstino, or assuming $\tilde{g} \to \tilde{\delta} q\bar{q}$ and the photino is short lived, we limit Λ_{ss}, the supersymmetry breaking parameter; and (3) assuming $\tilde{g} \to \tilde{\gamma} q\bar{q}$ dominates, we exclude photino lifetimes $\tau_{\tilde{\gamma}}/m_{\tilde{\gamma}}$ between about 10^{-10} and 1 sec/GeV. These limits are shown in Figs. 11 and 12.

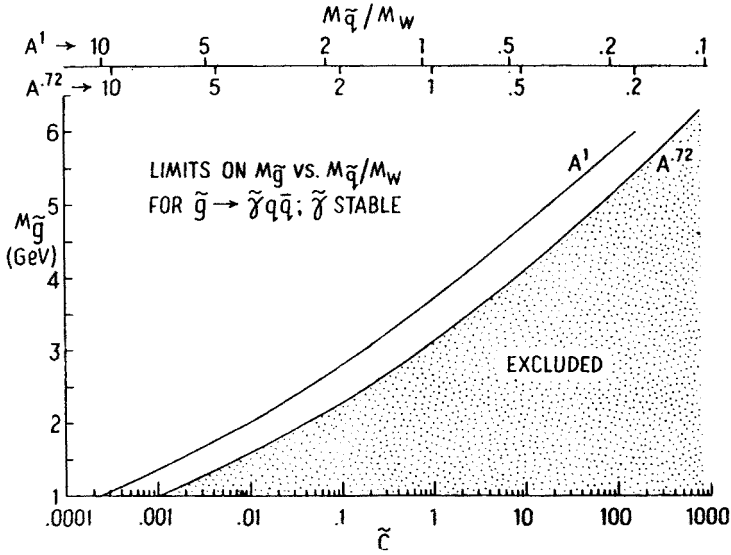

Fig. 11. $m_{\tilde{g}}$ vs $\tilde{c}$ for Case 1 ($\tilde{g} \rightarrow \tilde{\gamma} q\bar{q}$; $\tilde{\gamma}$ long lived and interacts in calorimeter with $\sigma = \tilde{c}E \times 10^{-38}$ cm^{-2}). 90% CL limits

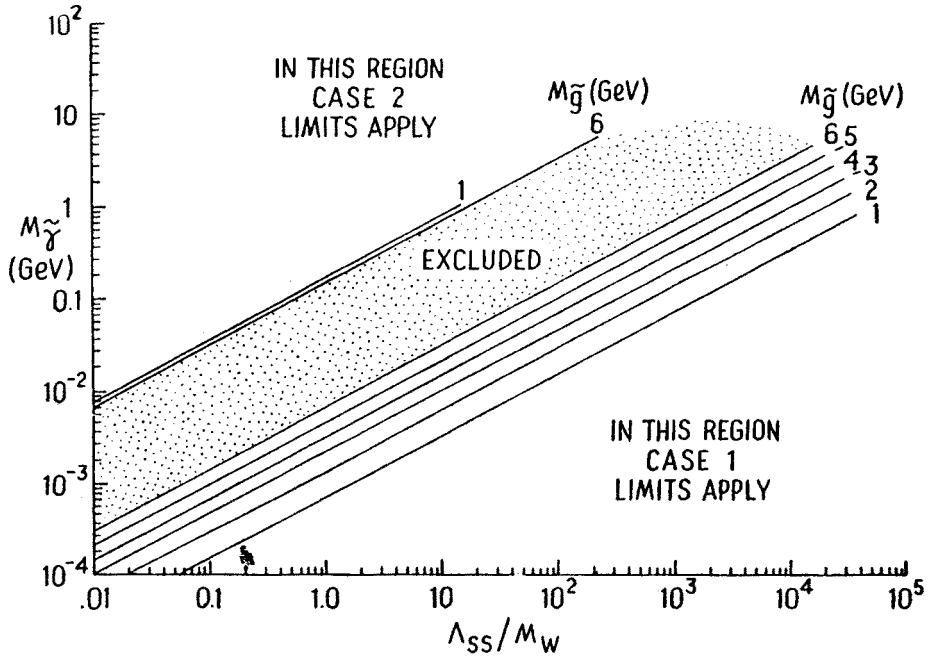

Fig. 12. $m_{\tilde{\gamma}}$ vs Λ_{ss} for Case 3 ($\tilde{g} \rightarrow \tilde{\gamma} q\bar{q}$; $\tilde{\gamma}$ decays in calorimeter and photon interacts. If the gluino mass and Λ_{ss}/m_W are in the cross-hatched region we should have observed $\tilde{\gamma}$ decays in our detector. The upper limits are essentially the same for $A^{0.72}$ or A^1 production cross section. The lower limits were drawn assuming $A^{0.72}$ production cross section. These limits would be a factor 1.27 lower for A^1)

REFERENCES

[1] P. Bosetti et al., *Phys. Lett.* **74B**, 143 (1978).
[2] M. Jonker et al., *Phys. Lett.* **96B**, 435 (1980).
[3] T. Hansl et al., *Phys. Lett.* **74B**, 139 (1978).
[4] J. L. Ritchie et al., *Phys. Rev. Lett.* **44**, 230 (1980).
[5] M. Aguilar-Benitez et al., CERN Report No. FP 82-204 (to be published).
[6] J. Irion et al., *Phys. Lett.* **99B**, 495 (1981).
[7] M. Basile et al., *Nuovo Cimento* **A63**, 230 (1981).
[8] D. Drijard et al., *Phys. Lett.* **85B**, 452 (1979).
[9] W. Lockman et al., *Phys. Lett.* **85B**, 443 (1979).
[10] P. Alibran et al., *Phys. Lett.* **74B**, 134 (1978).
[11] H. Fritzsch, *Phys. Lett.* **67B**, 217 (1977).
[12] F. Halzen, *Phys. Lett.* **69B**, 105 (1977); F. Halzen, S. Matsuda, *Phys. Rev.* **D17**, 1344 (1978).
[13] M. B. Einhorn, S. D. Ellis, *Phys. Rev.* **D12**, 2007 (1975).
[14] L. M. Jones, H. W. Wyld, *Phys. Rev.* **D17**, 1782 (1978).
[15] J. Babcock, D. Sivers, S. Wolfram, *Phys. Rev.* **D18**, 162 (1978).
[16] C. E. Carlson, R. Suaya, *Phys. Rev.* **D18**, 760 (1978).
[17] H. M. Georgi et al., *Ann. Phys.* (USA) **114**, 273 (1978).
[18] K. Hagiwara, T. Yoshino, *Phys. Lett.* **80B**, 282 (1979).
[19] B. L. Combridge, *Nucl. Phys.* **B151**, 429 (1979).
[20] C. E. Carlson, R. Suaya, *Phys. Lett.* **81B**, 329 (1980).
[21] R. Winder, C. Michael, *Nucl. Phys.* **B173**, 59 (1978).
[22] S. J. Brodsky et al., *Phys. Lett.* **93B**, 451 (1980).
[23] R. C. Ball et al., *Phys. Rev. Lett.* **51**, 743 (1983).
[24] J. G. de Groot et al., *Z. Phys.* **C1**, 143 (1979).
[25] M. Heagy et al., *Phys. Rev.* **D23**, 1045 (1981).
[26] H. W. Atherton et al., CERN Preprint 80-07.
[27] A. Barton et al., *Phys. Rev.* **D26**, 1497 (1982).
[28] P. Skubic et al., *Phys. Rev.* **D18**, 3115 (1978).
[29] Particle Data Group, Aguilar-Benitez et al., *Phys. Lett.* **111B**, 1 (1982). The neutral current cross section for lead was calculated using the ratio $\sigma(\nu n)/\sigma(\nu p)$ reported by Marriner et al., *Phys. Rev.* **D27**, 2569 (1983).
[30] E. S. Smith, Ph. D. Thesis, University of Wisconsin 1983.
[31] The method used was generally that described in Ref. [23] however a different fiducial volume was chosen.

Editorial note. This article was proofread by the editors only, not by the author.